ICES CM 2004 / N:12

Slope current in the Cantabrian: Observations and modeling of seasonal variability and interaction with Aviles Canyon.

Manuel Ruiz Villarreal, Henrique Coelho, Guillermo Díaz del Río, and João Nogueira

Manuel Ruiz Villarreal and Guillermo Diaz del Río: Instituto Español de Oceanografía (IEO), C.O. de A Coruña, Muelle de Animas, s/n, 15001 A Coruña, Spain. [tel: +34-981-205362 fax: +34-981-229077 e-mail: manuel.ruiz@co.ieo.es

Henrique Coelho Hidromod, Núcleo Central Taguspark, 349, 2780-920 Oeiras, Portugal

João Nogueira, MARETEC, Instituto Superior Técnico, Av Rovisco Lisboa, Portugal

Abstract

The Cantabrian shelf and slope are located in the southern part of the Bay of Biscay. They are part of an eastern boundary system (Canarias-Portugal), but the coastline orientation is EW, not NS. Seasonal evolution of hydrographic properties and evidences of mesoscale spatial variability are available in the literature. However, very scarce information about currents exists, apart from estimations from hydrographic campaigns and satellite imaginery. In this contribution, we will present a reanalysis of Eulerian measurements in the Cantabrian slope and shelf from February 1995 to February 1996. Three mooring lines were moored at three locations: slope (900 m), shelf (200 m) and Aviles canyon (500 m). The currents exhibit a clear seasonal signal, with poleward slope flow in winter months (peaks of 40-50 cm/s) at 75-150 m and westward (equatorward) slope flow during summer months. The currents show intense subtidal variability and also baroclinic effects are evident from the vertical structure. The data set allows to evaluate the effect of Aviles canyon on slope flow. In the "poleward" season, currents in the canyon follow the poleward main slope flow, while in the "equatorward" season currents at 75-150 m are directed upcanyon. Some numerical experiments with the hydrodynamical model MOHID (http://www.mohid.com) qualitatively reproduced the observed impact of the canyon on mean currents.

Keywords: Slope current, Cantabrian, poleward, canyon, upwelling, numerical model

1. Introduction

The Cantabrian Sea (figure 1) is the southern part of the Bay of Biscay, on the northern Spanish coast. The Portuguese-Galician coast from Cape San Vicente is roughly NS oriented until Finisterre cape. From there on, the coast bends to a EW orientation. From Ortegal promontory the slope is mainly EW oriented. The shelf is narrow and the slope is around 30 km from the coast. Several topographic accidents are found on the Cantabrian shelf and slope: it is intersected by a seamount (Le Danois Bank) after Cape Peñas and by several canyons (Aviles, Torrelavega, Santander, Cap Breton). Aviles canyon is located west of Cape Peñas and intersects the shelf and slope in a NE direction (about 45º from the EW direction). Its dimensions are 32 km long (from the isobath 1000 m in the direction of the slope to the 200 m isobath) and 15 km broad in the 200 m isobath.

The hydrology of waters in the Bay of Biscay has been reviewed by van Aken 2001. The first water mass found below the mixing layer is the Eastern North Atlantic Central Water (ENACW). Under ENACW, Mediterranean Water appears at a depth of around 1000 m. In the Cantabrian, the two cores of the MW north of San Vicente Cape are not observed. Seasonal evolution of hydrographic properties in the shelf and slope in the Bay of Biscay and evidences of mesoscale spatial variability are available in the literature (Lavin et al. 1998, Koutsikopoulos and Le Cann, 1996, Gil et al., 2002, Gil 2003). However, very scarce information about currents exists, apart from estimations from hydrographic campaigns and satellite imaginery.

The only report of Eulerian measurements in the Cantabrian shelf and slope is the paper by Pingree and Le Cann, 1990. They report a continuous poleward flow in the Bay of Biscay slopes. In the Cantabrian, they describe the results of a nine-month mooring from June 1988 to April 1989 (mooring 118 in their paper: 210 m, 481 m and 954 m) in a water depth of 1005 m west of Cape Ortegal (44º 1.9' N 6º 58.5' W). They found a seasonal variation of surface flows (inferred from the 210 m currentmeter) with eastward (poleward) current from October to March. Monthly mean values during these months are of 15 cm/s and maximum instantaneous along-slope currents of 60 cm/s. Currents during the other months (June to October 1988 and February to March 1989) are westward and means are typically of less than 5 cm/s. The currentmeter at 481 m measured weaker residual currents (2.8 cm/s) opposing the "subsurface" residual flow in some months. Mean currents at 954 m were marginally down-slope and weak. Winter flow is baroclinic and confined to the upper part of the water column. In their figure 3 they show daily values that show variability in surface flow with pulses, that they cannot clear correlate with atmospheric forcing although they report correlation with geostrophic wind direction (therefore Ekman transport) and periods of increased surface flows.

The accepted view of circulation in the Cantabrian from the above described information is that there are two phases of the flow associated with the variability of the prevailing winds: poleward flow in winter and equatorward flow in summer, with

spring and autumn transition seasons. Poleward flow in the Iberian slope is reported in winter, as north as in Armorican and Celtic slopes (Pingree and Le Cann, 1990, Frouin et al. 1990, Haynes and Barton, 1990, Garcia-Soto et al. 2002). During spring and summer, a westward flow in the shelf is obtained from geostrophic computations (Gil et al. 2002) especially for upwelling conditions, although a complex frontal structure from the coast to the slope related to upwelling has been measured in some cruises (Lavin et al. 1997, Gil et al. 2002) .

In this paper, we describe the main features of circulation deduced from the analysis of 3 lines of currentmeters deployed for 1 year in the shelf, slope and inside Aviles canyon. The impact of Aviles canyon on mean circulation is assessed. The results of the currentmeter analysis are compared to numerical simulations with MOHID (http://www.mohid.com).

2. Data set

The SEFOS project was aimed at determining the relationships between oceanography of the European shelf edge area and the distribution of some of the major commercial fish at all life history stages (Reid, 2001). In the Cantabrian, it included the mooring of 3 array of currentmeters in the Cantabrian shelf and slope (figure 2). This currentmeter set was compared to a numerical model by Bartsch et al. 1996 and some months of the currentmeter in the slope mooring at MW level (1000 m) were presented in Diaz del Rio et al. 1998. One of the mooring lines was located in the shelf (43º 36.8' N 6º 44.1'W, 200 m depth, ~5 km from the coast) to the west of the canyon, in a longitude close to the Navia river mouth. Other line was moored ~49 km eastwards in Aviles canyon near the center of the canyon (43º 45' N 6º 9.5'W, 500 m depth, ~20 km from the coast). The third line was moored on the slope to the east of the canyon (43º 57.8'N 5º 51.1'W, depth 1000m, ~21 km from the coast) at the longitude of Cape Peñas (~34 km offshore), and ~35 km from the canyon mooring. The slope in this area is oriented slightly NE-SW, with an angle of 20-30º from EW direction and it continues this NE direction towards Le Danois Bank. They were kept at those places for one year: February 1995 to February 1996, with 2 maintenance operations (May and September), that involved recovering the mooring line, reading and cleaning the currentmeters and mooring them again. Minimum depth for currentmeters was 75 m to avoid damage for fishing activities. On the shelf line, two currentmeters were moored at 74 and 80 m. In the canyon, currentmeters were placed at 75, 180 and 450 m. In the slope, 4 currentmeters were set at 75, 180,450 and 1000m. During the third phase of the measurement the 180 m currentmeter in the slope line did not work properly. Currentmeter were RCM7 and RCM8 Aanderaa currentmeters equipped with a temperature sensor. Data were adquired at a 30 minutes interval. Original data were filtered with a Godin type A2A2A3 moving average. The subtidal currents used in the paper were computed with a Godin A24A24A25 filter and subsampled every 6 hours.

3. The model

We have used the model MOHID, which was originally developed at the Instituto Superior Técnico (IST) in Lisbon. A detailed description of the model can be found in

Coelho *et al*, (2002). We have simulated the circulation over Aviles canyon using a series of nested models. The level 1 model is a regional model of the Northeast Atlantic with the same configuration described in Coelho et al. (2002). The level 2 is embedded in level 1 and is a local model for the Cantabrian Coast centered at Aviles Canyon. In the following, we describe the numerical model and the setting of the large and small scale nested models.

3.1. Equations

MOHID solves the three-dimensional primitive equations in Cartesian coordinates for incompressible flows. Hydrostatic equilibrium is assumed, as is as Boussinesq approximation. In the vertical MOHID uses a general coordinate.

Mass and momentum evolution equations are:

$$\frac{\partial u_i}{\partial x_i} = 0 \qquad (1)$$

$$\frac{\partial u_1}{\partial t} + \frac{\partial \left(u_j u_1\right)}{\partial x_j} = -fu_2 - g\frac{\rho_\eta}{\rho_0}\frac{\partial \eta}{\partial x_1} - \frac{1}{\rho_0}\frac{\partial p_s}{\partial x_1} - \frac{g}{\rho_0}\int_z^\eta \frac{\partial \rho'}{\partial x_1}dx_3 + \frac{\partial}{\partial x_j}\left(A_j \frac{\partial u_1}{\partial x_j}\right) \qquad (2)$$

$$\frac{\partial u_2}{\partial t} + \frac{\partial \left(u_j u_2\right)}{\partial x_j} = fu_1 - g\frac{\rho_\eta}{\rho_0}\frac{\partial \eta}{\partial x_2} - \frac{1}{\rho_0}\frac{\partial p_s}{\partial x_2} - \frac{g}{\rho_0}\int_z^\eta \frac{\partial \rho'}{\partial x_2}dx_3 + \frac{\partial}{\partial x_j}\left(A_j \frac{\partial u_2}{\partial x_j}\right) \qquad (3)$$

$$\frac{\partial p}{\partial x_3} = -\rho g \qquad (4)$$

Where u_i are the velocity vector components in Cartesian x_i directions positive to the east, to north and upward, η is the free surface elevation, f is the Coriolis parameter, A_i the turbulent viscosity and p_s is the atmospheric pressure. ρ is density and ρ' its anomaly. Density is calculated as a function of temperature and salinity by the equation of state presented by Millero e Poisson (1981).

The computed flow field transports salinity, temperature and other tracers using an advection-diffusion equation.

The model uses a semi-implicit ADI algorithm with two time levels per iteration. Two numerical schemes are currently implemented: the 4-equation S21 scheme (Abbott *et al*, 1973), and the 6-equation Leendertsee scheme (Leendertsee, 1967).

Free surface elevation is computed through integration of equation 4 over the water column. The two components of the horizontal velocity are globally centred in *t+1/2* leading to a second-order time accuracy. Vertical fluxes are also computed by continuity (considering the hydrostatic approach), integrating over each cell volume.

For horizontal diffusion of heat, salt and momentum, a choice can be made between Laplacian or biharmonic operators with constant coefficients. For this study the biharmonic operator proved to be more appropriate for the spatial scales involved. Bottom stress is parameterized using a quadratic law. Vertical eddy viscosity/diffusivity is determined using a turbulence closure model selected from those available in the General Ocean Turbulence Model (Burchard et al. 1990) incorporated in MOHID. In this study a simplified version of the model proposed by

Gaspar *et al* (1990) was used, since it gives reasonable results without excessively increasing use of CPU resources.

3.2 Experimental design and forcing of the large scale model

The model domain encompasses the west coasts of Iberia and Morocco, extending from 32ºN to 54ºN and from 0º to 30ºW. Horizontal grid spacing is 8.5 km in both directions. Bottom topography was derived from ETOPO2 by means of an interpolation for the model grid followed by smoothing with a five-point Laplacian filter. The bottom depth is then determined, using shaved cells. The model uses 18 vertical layers centered at constant z-levels at depths of 5, 20, 45, 80, 130, 200, 290, 400, 530, 680, 850, 1040, 1250, 1480, 1750, 2200, 3000 and 4250 m.

Biharmonic heat, salt and momentum diffusion coefficients are set to $2x10^9$ m^4s^{-1}, a value equal to the one used by Batteen *et al* (2000) with a similar horizontal resolution.

3.2.1 Lateral Boundary Conditions

Normal and tangential velocities are set to zero at the sidewalls. Fresh water river input at coastal boundaries is not considered in this study. The western, southern and northern boundaries are open, while the eastern boundary a sponge layer is used in the Mediterranean Sea. At the open boundaries we need some conditions for the prognostic variables: sea surface height, barotropic velocity, baroclinic velocity, temperature and salinity. The set of boundary conditions used is very similar to the FOA scheme conceived by Palma and Matano (2000). This scheme is basically the same as the one used by Oey and Chen (1992). It consists of imposing the barotropic transports at the open boundary that are consistent with the density field and at the same time allowing waves that are generated inside the domain to radiate out.

Barotropic velocities and sea surface height

The barotropic velocities at the open boundary are deduced from steady seasonal transports (the method of implementation is discussed below). Additionally, for the normal component of barotropic velocity ($\overline{u_n}$) we use a radiation condition proposed by Flather (1976):

$$\overline{u_n} = \overline{u_n^{c\lim}} - \sqrt{\frac{g}{H}}\left(\eta - \eta^{c\lim}\right) \quad (5)$$

This condition allows volume conservation and is very simple to apply.

Baroclinic velocities

Sommerfeld's one-dimensional radiation condition is applied for the normal baroclinic velocities at the boundary:

$$\frac{\partial \phi}{\partial t} \pm c_i \frac{\partial \phi}{\partial x} = -\frac{\phi}{\tau} \quad (6)$$

where ϕ stands for u and v, c_i is the fixed baroclinic internal wave speed, τ is a relaxation time scale and the plus (minus) sign applies to the right (left) open boundary. Equation (7) is solved using an implicit upstream method for the partial derivatives, and the internal wave speed is fixed at $\sqrt{gH \times 10^{-3}}$, where H is the local depth.

Scalars: temperature and salinity

Our boundary condition for scalars is exactly the same as the one proposed by Oey and Chen (1992):

$$\frac{\partial \phi}{\partial t} + u\frac{\partial \phi}{\partial x} = 0 \qquad (7)$$

where ϕ stands for temperature/salinity and $\frac{\partial \phi}{\partial x} \approx \frac{\phi - \phi_{c\lim}}{\Delta x}$ during inflow.

Along with this set of boundary conditions some of the prognostic variables are nudged to climatology by applying a nudging term in the prognostic equations near the open boundaries:

$$\frac{\partial \phi}{\partial t} = Advection + Diffusion + Sources - Sinks + \frac{1}{\tau}\left(\phi - \phi_{c\lim}\right) \qquad (8)$$

where ϕ stands for temperature, salinity barotropic and baroclinic components of velocity, τ is a relaxation time scale that varies smoothly from its value at the open boundary (180 days) to infinite within 100 km from the boundary. Finally ϕ_{clim} is the external value computed from climatological data.

In order to implement the set of boundary conditions described above we need to compute external values for the prognostics variables. For the scalars (temperature and salinity) the external data used is the same data used for model initializations at the boundary points that will be described below. The data is interpolated in time for the model time step allowing the boundary condition to be variable in time. To determine the barotropic velocities a level of no motion at 2500 m is assumed according to Paillet and Mercier (1997) and Arhan et al (1994). Knowing the depth mean currents and the density field, we calculated the external baroclinic velocities normal to the boundary by assuming the thermal wind relation. Finally, since barotropic transports are known, sea surface height is calculated from the vertically integrated geostrophic relation.

Initialization and Atmospheric Forcing

The model is initialized from rest with an horizontal sea surface. The climatological temperature and salinity fields are extracted from the new World Ocean Atlas with a ¼ of degree resolution (WOA01) and then interpolated for the model grid.

The spin-up phase consists of a 3-year run using monthly surface climatological momentum fluxes derived from the near-surface analysis of the European Center for Medium-Range Weather Forecasts ECMWF (Trenberth *et al*, 1990). After this period the volume-averaged kinetic energy is found to oscillate around an equilibrium value. Surface temperature and salinity are relaxed to climatological data during the spin-up phase. The data is interpolated spatially for the model grid and temporally for the model time step. During the entire run, temperature and salinity are relaxed to climatological by adding an adjustment term $[-A(z)(\phi - \phi_{c\lim})]$ to the right hand side of scalar equations (ϕ being the temperature or salinity, $\phi_{c\lim}$ its climatological value and $A(z)$ given by $A(z) = \frac{1}{\tau}\left[1 - \exp(z/\lambda)\right]$, with τ=270 days and τ=1000 m).

3.2.2. Experimental design and forcing of the small scale model

All the boundary conditions described for the large scale model are also used in the local model for the Cantabrian Coast. “Climatological” solutions needed for the open boundary conditions are obtained by interpolation of the solution of the large scale model. Major differences are: resolution of the small scale model is 2.5 km in both directions; relaxation time at the open boundary is 7 days going to infinite 20 km away from the boundary. Vertical levels are the same described for the large scale model.

4. Results

4.1 Observations

Stick plots of subtidal currents at the three mooring sites are shown in figure 3. Sticks are colored with the temperature measured by the currentmeter sensor. The first noticeable feature is the warming from October 95, that is associated with a mean eastward (poleward) flow at levels above 200 m. Poleward currents reach peaks of 40-50 cm s^{-1} in canyon and ocean currentmeters at 75 m. Although much variability is observed, this currentmeters above 200 m suggest an eastward flow from March to September. This is clearly observed in figures 4 and 5, where we plot the mean monthly currents at the mooring locations. In tables 1 to 3, monthly statistics of the hourly velocity data are provided together with temperature data. The direction of maximum variance is also given. From the inspection of mean currents, we can identify two phases of the flow: A poleward phase during the winter where the currents are eastward and strong, associated with the development of a surface poleward current along the western Iberian Coast; and an equatorward phase during the summer associated with the wind regime for that time of the year. During the equatorward phase upwelling episodes are frequent.

March to July monthly mean plots are characteristic of an “equatorward” phase. Monthly mean currents in the canyon and slope moorings are directed westwards at 75 m (with values of around 2.5 cm/s). At 180 m the difference between slope and canyon currents is stronger, with canyon currents clearly flowing upcanyon. At 450 m, there is also difference between slope and canyon currents although canyon currents are not intense. The 180 m vector at the slope also is directed westwards at the slope and it is oriented upcanyon at the canyon mooring. At 450 m the mean velocity is reduced and does not show a clear orientation. The values of the mean at 1000 m (MW level) is of the order of 1 cm/s ad is directed towards the NE roughly following the slope orientation for February to June, except in April. The currentmeter at the shelf (75 m) shows an eastward flow, except in March, where there is evidence of strong mesoscale activity from stick plots. Note the difference of scale in June, when eastward surface currents and also upcanyon currents are stronger.

For October to January, mean flow in the upper layers (75m and 180 m) is directed eastwards, therefore poleward. Maximum poleward velocities are in December and

January and reach peaks of 40-50 cm s^{-1} in canyon and slope currentmeters at 75 m. In November poleward velocities in the canyon currrentmeter at 75 m are very intense (see table): they are the maximum velocities in this phase (20.14 cm s^{-1}), but are only 4.99 cm s^{-1} at 180 m and not very intense at the 75 m slope currentmeter. The direction is more inshore than in December-February and from the stick plot figure we can also notice a warming at the end of October (in 75 m at slope and canyon) and again at the end of November in the 75m canyon currents. The flow at 450 in the canyon is variable but directed offshore. This suggest the existence of mesoscale activity near the currentmeter not related with the poleward current.

4.2 Model results

We have forced the model with a time-varying flow, but in this contribution we have decided to concentrate only on the analysis of mean circulation patterns. Therefore, we only present mean values of circulation for the two phases we have established from the currentmeter results. In figure 6 , we plot mean results of the model for the equatorward and poleward phases at 80, 200 and 400 m depth

During the equatorward phase, where upwelling episodes dominate, the mean pattern we find is a westward flow in surface layers coherent between slope and canyon. This westward velocity is more intense towards the coast and also from the slope seawards, where a coherent westward flow is seen in all layers. At 200 m, westward flow in the slope transforms into an upcanyon flow in the canyon, apparently more intense towards the west part of the canyon (therefore the downstream part). A cyclonic vortex at 400 m apparently dominates the circulation in the deeper layers in the canyon.

A poleward flow more intense onshore can be observed in the shelf and slope. This flow can be observed also in deeper layers, although in the canyon it is somewhat reduced in depth. From the slope onwards a westward flow seems to be characteristic, specially at 400 m and offshore. The canyon seems to increase offshore flow, specially on the downstream part of the canyon.

5. Discussion

The observed mean patterns of circulation roughly support the accepted schematic view of circulation in the Cantabrian: poleward flow in winter months and westward flow in spring-summer months. However, we have seen that variability is intense, both temporal and spatially. The poleward flow associated with the penetration of the Iberian Poleward Current in the Cantabrian is observed from December 1995. This flow is more intense in the shelf and shelf-break, in accordance with estimations from hydrographical cruises (see for example, fig. 5 in Gil 2003). In the 80 m model results in figure 6, a zone of reduced mean velocities is seen from the slope offshore, that can be related to mesoscale activity like that observed by Gil 2003 east from our zone in

December 1995. Equatorward flow is found on slope currentmeters and in 75 m canyon currentmeter during spring-summer. Westward residual flow is more intense than in the 210 m currentmeter of the mooring by Pingree and Le Cann, 1990, around 100 km west from the slope mooring. The interesting conclusion of our results is the impact of Aviles canyon on mean currents. We have seen that the impact of the canyon on circulation is more intense for the equatorward phase, when mean incident current is from the east and upwelling episodes in the west are more frequent. During this phase, the mean westward flow is transformed in upcanyon flow in the canyon, and therefore upwelling is enhanced, especially at 180 m. The shelf currentmeter shows intense variability with a mean eastward component in summer months and influence of IPC waters in winter months. This currentmeter is around 5 km from the coast and, apart from the influence of Navia run-off, it is in a zone with strong dynamics influenced by upwelling. Therefore, mean values are not much useful for studying the dynamics in this shelf currentmeter.

Literature on canyon circulation is sparse. Some observations on canyons in the NW American coast (Hickey, 1997, Allen et al. 2001) show that submarine canyons are regions of enhanced upwelling during upwelling favorable conditions and that interaction of alongshore flow with canyon topography is time-dependent. Numerical and theoretical studies have identified the internal Rossby deformation ratio Ro as a key parameter for the canyon to affect circulation. According to Klinck (1988), only narrow canyons, ie canyons with width smaller than half Ro, have a strong effect on circulation. This was further supported by She and Klinck 2002, that found with numerical simulations with Astoria canyon (NW American coast) dimensions, that stratifications inducing Ro of the order of the canyon width strongly influence circulation. A typical Rossby radius in the Cantabrian ranges from 10 to 17 km (Gil et al. 2002), therefore Ro is comparable to the width of the canyon (15 km in the 200 m isobath). The main picture of circulation during the upwelling season over Aviles canyon is consistent with the schematic circulation established from observations during upwelling conditions in Astoria canyon (Hickey, 1997) and Barkley canyon (Allen et al. 2001). Numerical simulations with dimensions those of Astoria canyon (She and Klinck, 2000) support the conclusions of the previous studies. However, the previous studies, especially Hickey, 1997, reveal the strong variability of flow over the canyon with spatial gradients inside the canyon and temporally-varying response to the development and relaxation of upwelling pulses. Our data set was not intended to study the circulation over Aviles canyon, but to get a picture of mean currents in the Cantabrian.

Circulation in the Cantabrian exhibits a marked interannual variation (Lavin et al. 1996, Cabanas et al. 2003, Garcia-Soto et al. 2002, González-Pola et al. 2003). The most evident interannual variation is the extension of the Iberian Poleward Current in the Cantabrian, with some years when warm waters transported by the IPC are seen in the Cantabrian. The surface signature of IPC in thermal satellite images can be seen in the Cantabrian around Christmas, and therefore years with intense IPC penetration in the Cantabrian are named Navidad years. The autumn-winter 94-95 was not a year of marked Navidad, while the autumn-winter 95-96 was a strong Navidad year. The subsurface signature of this intense poleward flow in 95-96 is evident in our measurements. The subsurface signature in velocity and temperature was also seen in

Pingree and Le Cann, 1990 currentmeters in a year of weak Navidad (1988-1989).

Another factor that has to be taken into account for interpreting our measurements and putting the mean into a longer-term context is variability in rainfall. Winter 1994-1995 (from December to March) and 1995-1996 winter were particularly wet (Lavin et al. 1997) and low surface surface salinities compared to other years were measured at Santander standard section (Lavin et al. 1997). The currentmeter in the shelf is located very close to the mouth of the Navia river, with a mean monthly run-off in winter months that can reach more than 200 m^3s^{-1}. From December to March 1996 run-off was well above average, specially on January, when a mean monthly run-off of 535 m^3s^{-1} was measured (compared to a long-term January mean of 300 m^3s^{-1}). Also January to March 1995 values of monthly Navia run-off were very high, specially on March 1995, when monthly run-off reached 440 m^3s^{-1}(long term mean in March 200 m^3s^{-1}). Our model simulations did not consider river run-off and therefore cannot be used for interpreting the results of the shelf mooring.

Finally, the results of the currentmeter at 1000 m in the slope, show eastwards velocities of about 2-3 cm/s, apparently in the direction of the slope . The current-meter at 1000 m in Pingree and Le Cann, 1990 measured eastward velocities about 2-3 cm s^{-1} for a consecutive year about 8ºW. We have not analyzed the results of the numerical model at MW levels, since there are numerical problems in the parameterization of the MW spreading in numerical simulations (for example, Papadakis et al. 2004). In Coelho et al. 2001, a discussion on the representation of MW in our Atlantic domain is given.

6. Conclusions

In this contribution, we are able to summarize the mean circulation patterns in this zone of the Cantabrian and establish two dominant regimes that follow the variation of prevailing winds: a poleward phase and an equatorward phase (see schema in figure 7). During the poleward phase, beginning in October and reaching maximum values of poleward flow from December on, the incident flow in the canyon is from the west and it is more intense at the slope-edge from the coast. The flow is not strongly affected by the canyon and poleward flow is seen in all layers, with a maximum in the slope. Circulation in deeper layers of the canyon suggest an anticyclonic vortex. The mean pattern characteristic of the equatorial phase, that starts in March and when upwelling episodes are predominant, consists in an eastward flow in surface layers, with currents over the canyon and the slope well correlated. At 200 m, eastward flow in the slope (correlated with 75 m flow in the slope) takes an upcanyon direction over the canyon, therefore enhancing upwelling. The currents at 450 m are consistent with the existence of a cyclonic vortex. Although we have only concentrated on mean patterns, this picture is consistent with experimental and numerical results in canyons in the North-West Pacific coast (Hickey, 1997, Allen et al. 2001, She and Klinck, 2000), also subjected to seasonal upwelling.

Combining data-set and model results we have put forward mean circulation patterns. We are aware of the spatial and temporal variability of circulation over canyons, and

that our data-set was not intended to resolve this variability. However, we can extract valuable information on currents in this area where few published information is available. The study of short-term variability in currentmeter moorings and the comparison to local wind data sets to determine the time of upwelling pulses can help us in deepening our understanding of the impact of the canyon on circulation. This is also true for the analysis of the model simulations, although they have been forced with a large scale atmospheric climatology that might not resolve the local spatial and temporal variability of winds. Our results imply that studies of circulation and its impact on the ecosystem in the Cantabrian should take into account the strong influence of the canyon in circulation. Some studies have clearly shown the impact of canyons on phytoplankton and zooplankton and related it to the impact of canyon on circulation (Allen et al. 2001). In the vicinity of Aviles canyon, the results of a 7 day cruise in May 1996 indicate an increased primary production at the head of the canyon and the authors discuss the impact of this in zooplankton (Gonzalez-Quirós et al. 2003), although the limited physical information and the variability during the 7 days of the cruise does not allow to elucidate the role of the canyon, apart from the enhancement of upwelling suggested by our measurements.

Acknowledgements

Manuel Ruiz Villarreal is supported by a Ramon y Cajal fellowship (Ministerio de Ciencia y Tecnologia, Spain). The mooring line deployment was supported by the SEFOS project. We thank David Marcote for assistance in the acquisition of the data. The reanalysis of this data-set is performed in relation with VACLAN project. Model simulations were done in relationship to EUROSTRATAFORM project.

Month	*U*	*Std*	*V*	*Std*	*T*	*Std*	*Principal axis angle*
Shelf.	***Depth=***	***74 m***					
Jan	*2.51*	*6.09*	*-0.48*	*2.81*	*14.85*	*0.19*	*-14.90*
Feb	*-0.61*	*12.04*	*0.47*	*6.49*	*14.13*	*0.70*	*-23.61*
Mar	*-0.34*	*8.07*	*-0.19*	*4.18*	*12.72*	*0.34*	*-20.13*
Apr	*1.63*	*5.59*	*-0.87*	*2.39*	*12.01*	*0.12*	*-7.58*
May	*1.97*	*6.59*	*0.17*	*4.71*	*12.37*	*0.43*	*-14.40*
Jun	*2.50*	*4.98*	*-0.88*	*3.29*	*12.09*	*0.48*	*-21.02*
Jul	*1.85*	*5.64*	*-0.11*	*5.34*	*12.21*	*0.34*	*-39.32*
Aug	*2.09*	*5.44*	*-0.42*	*4.61*	*12.19*	*0.18*	*-26.92*
Sep	*0.70*	*10.04*	*0.71*	*9.10*	*13.18*	*0.95*	*-31.71*
Oct	*5.51*	*9.28*	*-0.11*	*10.25*	*13.26*	*0.45*	*-70.86*
Nov	*4.84*	*7.88*	*-0.23*	*4.73*	*14.81*	*0.77*	*-19.15*
Dec	*1.46*	*6.77*	*-0.56*	*2.63*	*14.97*	*0.59*	*-11.19*
Shelf.	***Depth=***	***80 m***					
Jan	*2.55*	*8.58*	*-0.17*	*4.35*	*14.86*	*0.23*	*-10.41*
Feb	*-1.69*	*10.82*	*0.68*	*5.61*	*14.19*	*0.79*	*-19.59*
Mar	*-0.60*	*8.20*	*-0.42*	*3.65*	*12.67*	*0.38*	*-16.89*
Apr	*1.40*	*6.18*	*-1.06*	*2.40*	*11.93*	*0.10*	*-8.95*
May	*1.32*	*6.71*	*0.76*	*5.00*	*12.27*	*0.39*	*-8.89*
Jun	*2.36*	*5.05*	*-1.46*	*3.30*	*11.98*	*0.43*	*-19.10*
Jul	*1.08*	*6.00*	*0.25*	*5.54*	*12.07*	*0.27*	*-33.45*
Aug	*1.26*	*4.88*	*0.17*	*4.27*	*12.08*	*0.14*	*-25.74*
Sep	*0.55*	*9.67*	*0.62*	*8.87*	*12.92*	*0.85*	*-30.17*
Oct	*4.29*	*9.03*	*0.32*	*9.97*	*13.04*	*0.41*	*-75.46*
Nov	*4.31*	*7.37*	*0.23*	*4.36*	*14.71*	*0.80*	*-12.92*
Dec	*1.73*	*7.54*	*-0.74*	*3.08*	*14.83*	*0.63*	*-8.62*

Table 1: Monthly mean statistics for currentmeters at the shelf mooring (43º 36.8' N 6º 44.1'W, 200 m depth)

Month	*U*	*Std*	*V*	*Std*	*T*	*Std*	*Principal axis angle*
Canyon.	***Depth=***	***75 m***					
Jan	*14.40*	*12.78*	*0.28*	*6.18*	*15.01*	*0.24*	*-1.92*
Feb	*3.29*	*11.59*	*-1.36*	*5.25*	*13.78*	*0.91*	*9.09*
Mar	*-3.99*	*9.51*	*-2.55*	*5.91*	*12.66*	*0.17*	*20.06*
Apr	*-4.88*	*6.66*	*-3.26*	*6.02*	*12.45*	*0.13*	*-29.24*
May	*-2.03*	*7.12*	*-2.52*	*5.63*	*12.67*	*0.25*	*-13.60*
Jun	*-2.97*	*7.42*	*-2.93*	*5.92*	*12.40*	*0.18*	*-3.49*
Jul	*-0.43*	*6.22*	*-1.97*	*5.41*	*12.30*	*0.22*	*6.54*
Aug	*0.02*	*6.00*	*-1.67*	*5.11*	*12.18*	*0.20*	*-4.26*
Sep	*-1.78*	*10.67*	*-1.22*	*5.78*	*13.29*	*0.79*	*5.16*
Oct	*2.05*	*11.09*	*1.22*	*10.79*	*14.23*	*1.26*	*-26.95*
Nov	*20.14*	*12.77*	*-0.09*	*9.22*	*14.86*	*0.62*	*-13.89*
Dec	*13.63*	*14.31*	*-0.56*	*6.29*	*14.85*	*0.56*	*3.87*
Canyon.	***Depth=***	***150 m***					
Jan	*11.05*	*12.41*	*0.07*	*6.95*	*14.75*	*0.50*	*-9.10*
Feb	*1.22*	*12.37*	*-1.59*	*6.46*	*13.39*	*0.90*	*-7.72*
Mar	*2.06*	*7.83*	*-1.93*	*5.78*	*12.03*	*0.30*	*1.28*
Apr	*1.23*	*6.24*	*-2.90*	*4.92*	*11.81*	*0.17*	*-14.55*
May	*1.92*	*4.88*	*-1.28*	*4.68*	*11.93*	*0.11*	*-35.47*
Jun	*5.13*	*5.73*	*-1.73*	*5.29*	*11.64*	*0.14*	*-26.92*
Jul	*2.78*	*4.96*	*-1.37*	*4.07*	*11.68*	*0.12*	*-14.85*
Aug	*1.81*	*4.57*	*-0.50*	*4.20*	*11.59*	*0.08*	*-5.39*
Sep	*1.72*	*4.85*	*-1.93*	*3.47*	*11.68*	*0.10*	*1.93*
Oct	*7.73*	*6.27*	*-1.23*	*4.45*	*11.85*	*0.22*	*-19.94*
Nov	*4.99*	*9.22*	*-0.04*	*6.43*	*12.94*	*0.51*	*-13.18*
Dec	*11.94*	*13.08*	*-0.81*	*5.37*	*13.44*	*0.83*	*1.67*
Canyon.	***Depth=***	***450 m***					
Jan	*-0.06*	*7.00*	*1.51*	*6.33*	*11.41*	*0.26*	*-40.81*
Feb	*1.52*	*7.31*	*0.94*	*7.10*	*11.07*	*0.20*	*-43.75*
Mar	*0.78*	*6.42*	*-0.05*	*7.15*	*10.95*	*0.17*	*-50.47*
Apr	*1.88*	*5.04*	*-0.27*	*6.52*	*11.04*	*0.12*	*-58.08*
May	*0.98*	*4.95*	*0.38*	*6.15*	*11.03*	*0.12*	*-55.44*
Jun	*4.15*	*4.86*	*-0.72*	*7.05*	*10.83*	*0.13*	*-62.16*
Jul	*0.56*	*3.30*	*0.43*	*4.49*	*11.09*	*0.12*	*-59.57*
Aug	*0.48*	*4.57*	*0.48*	*5.97*	*10.90*	*0.11*	*-57.42*
Sep	*1.15*	*5.69*	*0.05*	*6.44*	*11.00*	*0.24*	*-51.12*
Oct	*-1.42*	*3.92*	*1.08*	*5.38*	*11.28*	*0.31*	*-62.42*
Nov	*1.03*	*6.28*	*0.94*	*6.13*	*11.51*	*0.24*	*-43.68*
Dec	*-0.67*	*7.48*	*1.60*	*6.75*	*11.57*	*0.50*	*-40.32*

Table 2: Monthly mean statistics for currentmeters at the canyon mooring (43º 45' N 6º 9.5'W, 500 m depth)

Month	***U***	***Std***	***V***	***Std***	***T***	***Std***	***Principal axis angle***
Slope.	***Depth=***	***75 m***					
Jan	*21.27*	*15.63*	*7.18*	*9.02*	*14.57*	*0.48*	*-5.74*
Feb	*-0.24*	*12.24*	*0.38*	*7.12*	*13.31*	*0.68*	*-0.97*
Mar	*-5.40*	*12.60*	*-1.80*	*9.07*	*12.53*	*0.10*	*-10.41*
Apr	*4.70*	*10.93*	*2.48*	*7.23*	*12.41*	*0.08*	*-2.38*
May	*-3.56*	*9.24*	*0.17*	*7.41*	*12.41*	*0.10*	*-14.82*
Jun	*-8.90*	*8.23*	*1.10*	*7.21*	*12.23*	*0.10*	*-15.16*
Jul	*-1.46*	*8.16*	*-1.77*	*6.32*	*12.27*	*0.08*	*-12.17*
Aug	*-8.62*	*10.67*	*-0.57*	*7.46*	*12.29*	*0.10*	*-12.22*
Sep	*-2.73*	*10.97*	*1.14*	*10.70*	*15.03*	*1.78*	*-40.65*
Oct	*6.49*	*14.52*	*-0.08*	*13.26*	*16.22*	*1.07*	*5.70*
Nov	*8.04*	*10.65*	*1.08*	*9.82*	*15.74*	*0.81*	*30.00*
Dec	*12.96*	*13.70*	*2.73*	*8.63*	*14.55*	*0.30*	*6.42*
Slope.	***Depth=***	***180 m***					
Jan	*0.00*	*0.00*	*0.00*	*0.00*	*13.86*	*0.53*	*0.00*
Feb	*-6.35*	*6.15*	*-1.97*	*5.20*	*12.83*	*0.40*	*2.51*
Mar	*-5.17*	*10.27*	*-1.68*	*6.54*	*12.18*	*0.23*	*-8.27*
Apr	*4.52*	*8.38*	*0.90*	*4.32*	*11.80*	*0.10*	*-1.99*
May	*-3.19*	*8.12*	*-0.40*	*5.60*	*11.87*	*0.08*	*-13.86*
Jun	*-8.29*	*6.38*	*0.68*	*5.32*	*11.68*	*0.08*	*-6.88*
Jul	*-2.90*	*5.89*	*-2.11*	*4.52*	*11.72*	*0.06*	*-18.52*
Aug	*-7.34*	*8.67*	*-0.57*	*5.57*	*11.69*	*0.09*	*-8.97*
Sep	*-8.20*	*5.44*	*8.21*	*3.76*	*11.80*	*0.12*	*-11.24*
Oct	*0.00*	*0.00*	*0.00*	*0.00*	*11.87*	*0.12*	*0.00*
Nov	*0.00*	*0.00*	*0.00*	*0.00*	*12.43*	*0.28*	*0.00*
Dec	*0.00*	*0.00*	*0.00*	*0.00*	*12.76*	*0.69*	*0.00*
Slope.	***Depth=***	***450 m***					
Jan	*1.89*	*8.02*	*-0.89*	*5.29*	*11.21*	*0.14*	*9.55*
Feb	*-11.14*	*8.12*	*-5.29*	*5.29*	*11.10*	*0.11*	*12.32*
Mar	*0.66*	*9.92*	*-0.64*	*7.47*	*10.81*	*0.11*	*8.39*
Apr	*6.34*	*11.11*	*0.54*	*6.83*	*10.90*	*0.12*	*19.70*
May	*-1.25*	*6.74*	*0.90*	*6.40*	*10.89*	*0.10*	*35.49*
Jun	*-1.23*	*8.38*	*-1.89*	*6.60*	*10.75*	*0.07*	*-4.20*
Jul	*-1.89*	*5.33*	*-1.23*	*4.42*	*10.89*	*0.07*	*7.13*
Aug	*-1.95*	*8.45*	*0.69*	*6.62*	*10.79*	*0.09*	*8.66*
Sep	*-2.12*	*5.14*	*-0.39*	*6.16*	*10.96*	*0.13*	*68.16*
Oct	*6.58*	*5.77*	*0.09*	*5.24*	*10.98*	*0.11*	*-15.66*
Nov	*1.49*	*5.42*	*-0.98*	*5.24*	*11.14*	*0.10*	*-26.92*
Dec	*0.68*	*7.26*	*-0.82*	*7.48*	*11.19*	*0.19*	*51.22*
Slope.	***Depth=***	***1000 m***					
Jan	*0.86*	*5.28*	*-0.02*	*4.43*	*9.88*	*0.16*	*26.60*
Feb	*0.00*	*7.21*	*1.07*	*6.06*	*9.62*	*0.19*	*-29.30*
Mar	*1.00*	*6.92*	*1.15*	*8.72*	*9.51*	*0.22*	*-61.82*
Apr	*1.63*	*7.87*	*1.98*	*8.41*	*9.50*	*0.25*	*-51.45*

Month	***U***	***Std***	***V***	***Std***	***T***	***Std***	***Principal axis angle***
May	*-1.13*	*6.70*	*0.08*	*9.01*	*9.30*	*0.26*	*-61.06*
Jun	*0.24*	*6.21*	*1.13*	*8.44*	*9.46*	*0.25*	*-59.91*
Jul	*0.37*	*5.44*	*1.14*	*7.95*	*9.53*	*0.16*	*-62.70*
Aug	*-0.20*	*5.86*	*0.50*	*7.92*	*9.52*	*0.21*	*-70.71*
Sep	*0.11*	*6.61*	*0.21*	*7.35*	*9.64*	*0.19*	*-50.16*
Oct	*1.51*	*5.89*	*-0.03*	*6.29*	*9.93*	*0.19*	*-48.86*
Nov	*1.63*	*4.98*	*0.57*	*5.24*	*10.08*	*0.10*	*-49.99*
Dec	*1.55*	*4.76*	*0.60*	*4.51*	*9.97*	*0.10*	*-27.31*

References

- Abbot M.B., Damsgaardand A., Rodenhuis G.S., System 21, Jupiter, a design system for two-dimensional nearly-horizontal flows, J. Hyd. Res. 1 (1973) 1-28.
- Allen, S.E., C. Vindeirinho, R.E. Thomson, M.G.G. Foreman, and D.L. Mackas, Physical and biological processes over a submarine canyon during an upwelling event, Can. J. Fish. Aquat. Sci./J. Can. Sci. Halieut. Aquat. 58(4): 671-684 (2001).
- Arhan, M., Colin de Verdi×re, A, and L. Memery, The Eastern boundary of the subtropical North Atlantic, J. Phys. Oceanogr., 24, 1295-1316, 1994
- Bartsch, A. Lavin, L. Motos, A numerical model system of the region around the Iberian Peninsula: Model validation and application to hake larvae drift in the Bay of Biscay, ICES CM 1996.
- Batteen, M. L., J. R. Martinez, D. W. Bryan e E. J. Buch, 2000: A modeling study of the coastal eastern boundary current system off Iberia and Morocco, J. Geophys. Res., 105, 14173-14195.
- Burchard, H., K. Bolding and M.R.Villarreal, 1999, GOTM, a General Ocean Turbulence Model. Theory, implementation and test cases, European Commission, EUR 18745, 103 pp. 1999. See also GOTM website, http://www.gotm.net
- Cabanas, JM, A. Lavin, M.J. Garcia, C. Gonzalez-Pola, E. Tel Pérez, Oceanographic variability in the northern shelf of the Iberian Peninsula (southern Bay of Biscay), ICES Marine Science Symposium, in press, 2003.
- Coelho, H., R. Neves, M. White, P. Leitão and A. Santos: A Model for Ocean Circulation on the Iberian Coast. Journal of Marine Systems, accepted, 2001
- Diaz del Rio, G., N. Gonzalez, and D. Marcote, The intermediate Mediterranean water inflow along the northern slope of the Iberian Peninsula, *Oceanol. Acta*, 21 (2), 157-163, 1998.
- Flather, R.A., 1976: A tidal model of the northwest European continental shelf. Mem. Soc. R. Sci. Liege, Ser. 6(10), 141-164.
- Frouin, R., Fiúza, A.F.G., Ambar, I., Boyd, T.J., (1990) Observations of a poleward current off the coasts of Portugal and Spain during winter. Journal of Geophys. Res.. 95(C1):679–691.
- Fiuza, A.F.G., Hamann M., Ambar I., Días del Río G., González N., Cabanas, J.M., (1998). Water masses and their circulation off western Iberia during May 1993. Deep–Sea Res. I, 45:1127–1160.
- Garcia-Soto, C., R. D. Pingree, and L. Valdés, Navidad development in the southern Bay of Biscay: Climate change and swoddy structure from remote sensing and in situ measurements, *J. Geophys. Res.*, *107*(C8), 10.1029/2001JC001012, 2002
- Gil, J. Changes in the pattern of water masses resulting from a poleward slope current in the Cantabrian Sea (Bay of Biscay), Estuarine Coastal and Shelf Science 2003
- Gil, J., L . Valdés, M . Moral, R . Sánchez and C. García-Soto. (2002). Mesoscale variability in a high resolution grid in the Cantabrian Sea (southern Bay of Biscay). May 1995. Deep-Sea Research I. 49(9): 1591-1607
- González-Pola, C., A. Lavín and M. Vargas-Yañez, Intense warming and salinity modification of intermediate water masses in the southeastern corner of the Bay of

Biscay for the period 1992-2003, to appear in Journal of Geophysical Research.

- Gonzalez-Quirós, R., J. Cabal, F. Álvarez-Marqués and A. Isla, Ichthyoplankton distribution and plankton production related to the shelf break front at the Aviles canyon, ICES Journal of Marine Science, 60, 198-210, 2003.
- Haynes, R., E.D. Barton (1990). A poleward flow along the Atlantic coast of the Iberian Peninsula. J. of Geophys. Res, 95: 11425–11441.
- Hickey , B.M., The response of a steep-sided narrow canyon to strong wind forcing, J. Phys. Oceanography, 27, 697-726, 1997
- Koutsikopoulos and Le Cann, Physical processes and hydrological structures related to the Bay of Biscay anchova. Scientia Marina, 60(2), 9-19, 1996.
- Lavin, A., L. Valdes, J. Gil, M. Moral, 1998, Seasonal and inter-annual variability in the properties of surface water off Santander, Bay of Biscay, 1991-1995. Oceanologica Acta, 21, 179-190
- Leendertsee, J.J. and Liu, S.K 1978. A three-dimensional turbulent energy model for non-homogeneous estuaries and coastal sea systems. In J.C.J. Nihoul (Ed.), *Hydrodynamics of Estuaries and Fjords*: 387-405. Amsterdam: Elsevier.
- Millero, F. J. e A. Poisson, 1981: International one atmosphere equation of state for sea-water. Deep-Sea Research, 28, 624-629.
- Oey, L. e P. Chen, 1992. A Model Simulation of Circulation in the Northeast Atlantic Shelves and Seas. J. Geophys. Res., 97, 20,087-20,115.
- Paillet, J. and H. Mercier, 1997. An inverse model of the eastern North Atlantic general circulation and thermocline ventilation. Deep Sea Res., 44 (8), 1293-1328.
- Palma, E. D. and R. P. Matano, 2000: On the implementation of passive open boundary conditions for a general circulation model: The three-dimensional case. Journal of Geophysical Research, 105,. 8605-8627 (2000).
- Papadakis, M. P., E. P. Chassignet, and R.W. Hallberg, 2003: Numerical simulations of the Mediterranean sea outflow: Impact of the entrainment parameterization in an isopycnic coordinate ocean model. Ocean Modelling, 5(4), 325-356.
- Pingree R.D. and B. Le Cann, Structure, strength and seasonality of the slope currents in the Bay of Biscay region.
- Reid, SEFOS-shelf edge fisheries and oceanography studies: an overview, Fisheries Research, 50, 1-15, 2001
- Sánchez, F. and Gil, J. Hydrographic mesoscale structures and poleward current as a determinant of hake (Merluccius merluccius) recruitment in southern Bay of Biscay, ICES Journal of Marine Science, 57, 152-170, 2000.
- She, J. and J.M. Klinck, Flow near submarine canyons driven by constant winds, Journal of Geophysical Research, 105,C12, 28671-28694, 2000.
- Trenberth, K. E., W. G. Large e J. G. Olsen, 1990: The mean annual cycle in global wind stress. J. Phys. Oceanogr., 20, 1742-1760.
- Vitorino, J., A. Oliveira, J.M. Jouanneau and T. Drago, Winter dynamics on the northern Portuguese shelf. Part 1: Physical Processes, Progress in Oceanography, 52, 129-153, 2002
- H.M. van Aken (2001) The hydrography of the mid-latitude Northeast Atlantic Ocean - Part III, The thermocline water masses. Deep-Sea Research I, 48, 237-267

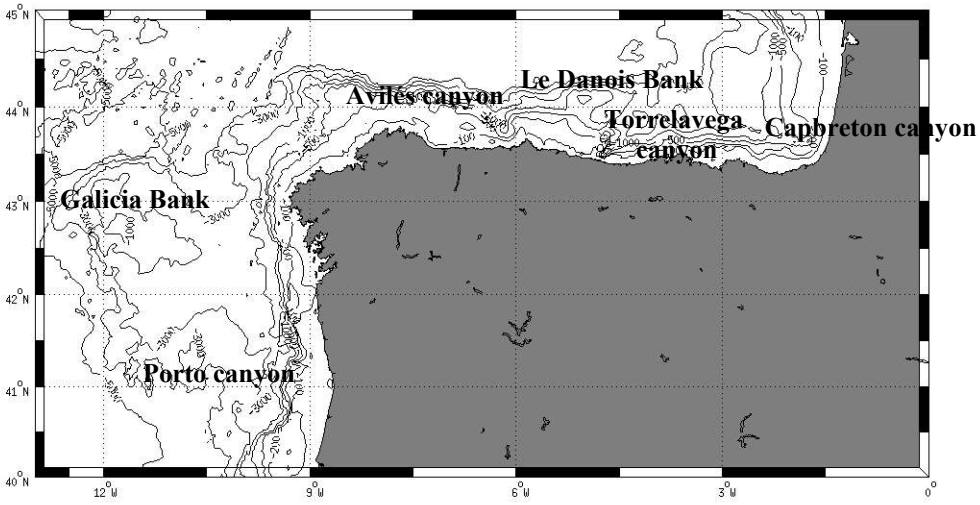

Figure 1: Geographical location of Aviles Canyon in the Cantabrian Sea.

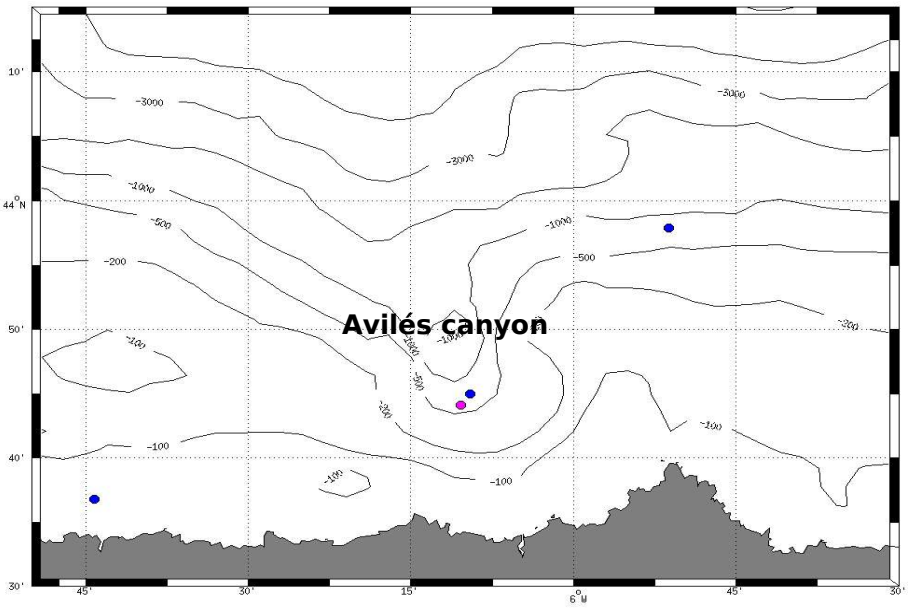

Figure 2: Topography and location of mooring lines around Aviles Canyon. The magenta circle corresponds to the location of a mooring line by Puertos del Estado since 1998.

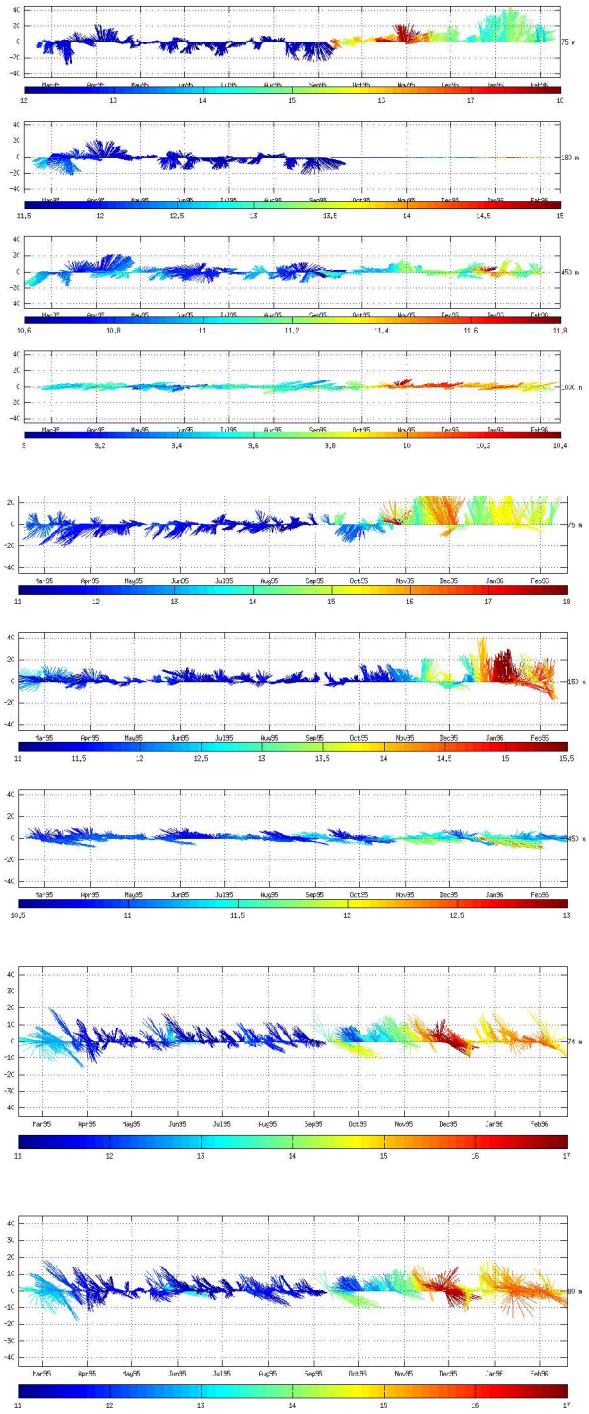

Figure 3: Stick plot of subtidal currents in slope, canyon and shelf. Temperature is plotted as a color scale.

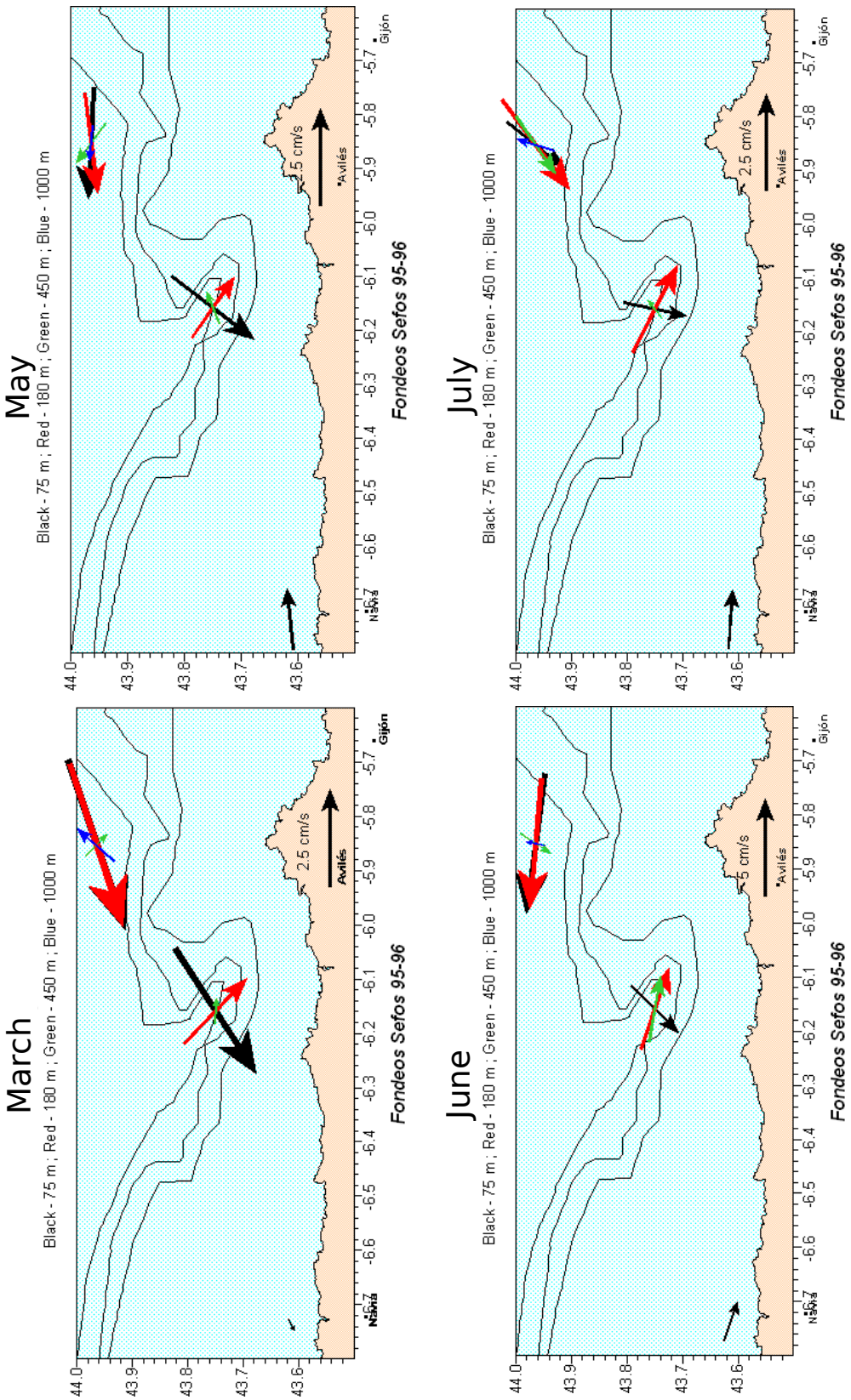

Figure 4: Monthly mean currents for months during the "equatorward" phase. Note the difference in scale between March-July and April-June.

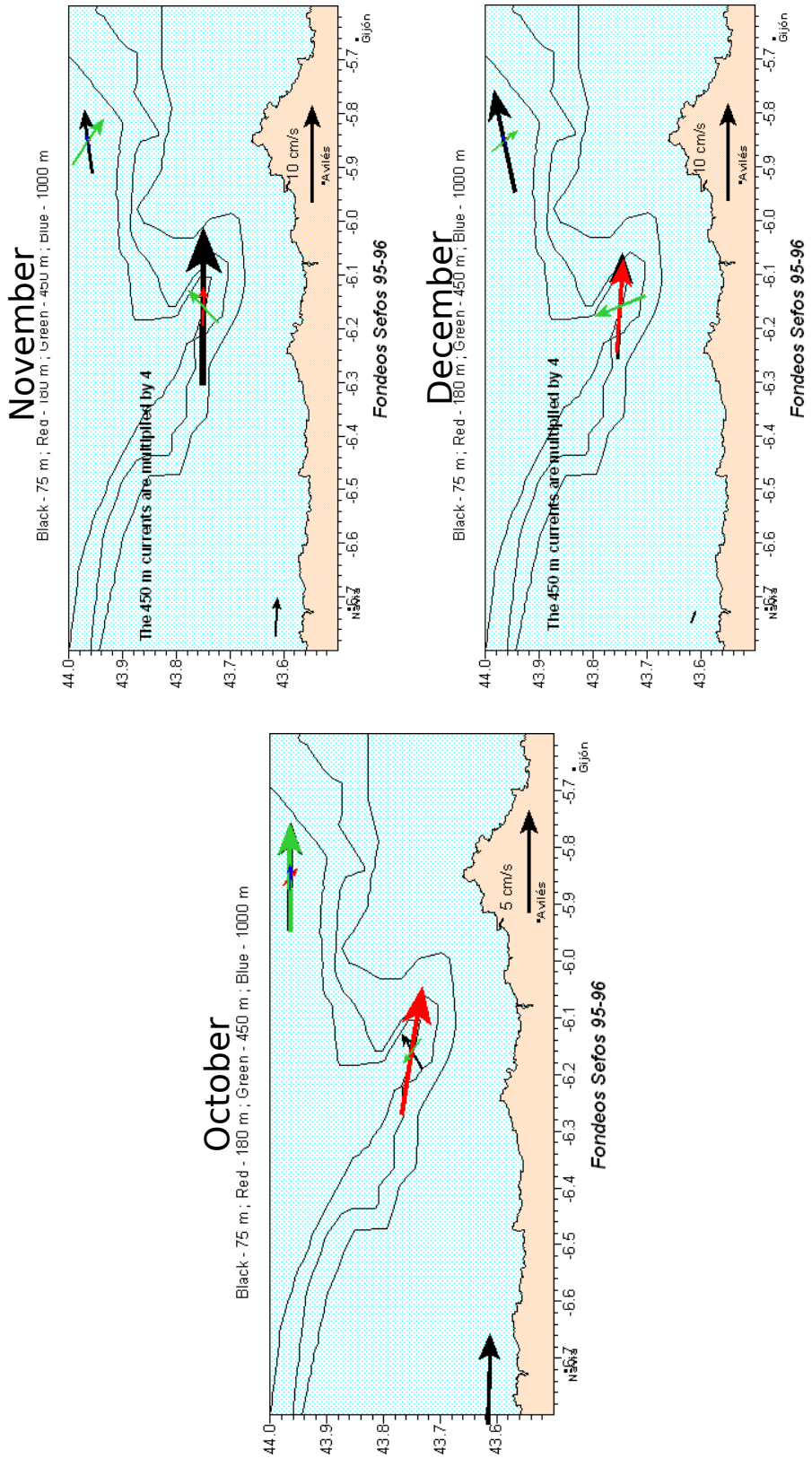

Figure 5: Monthly mean currents for months during the "poleward" phase. Note the difference in scale between October and the other plots.

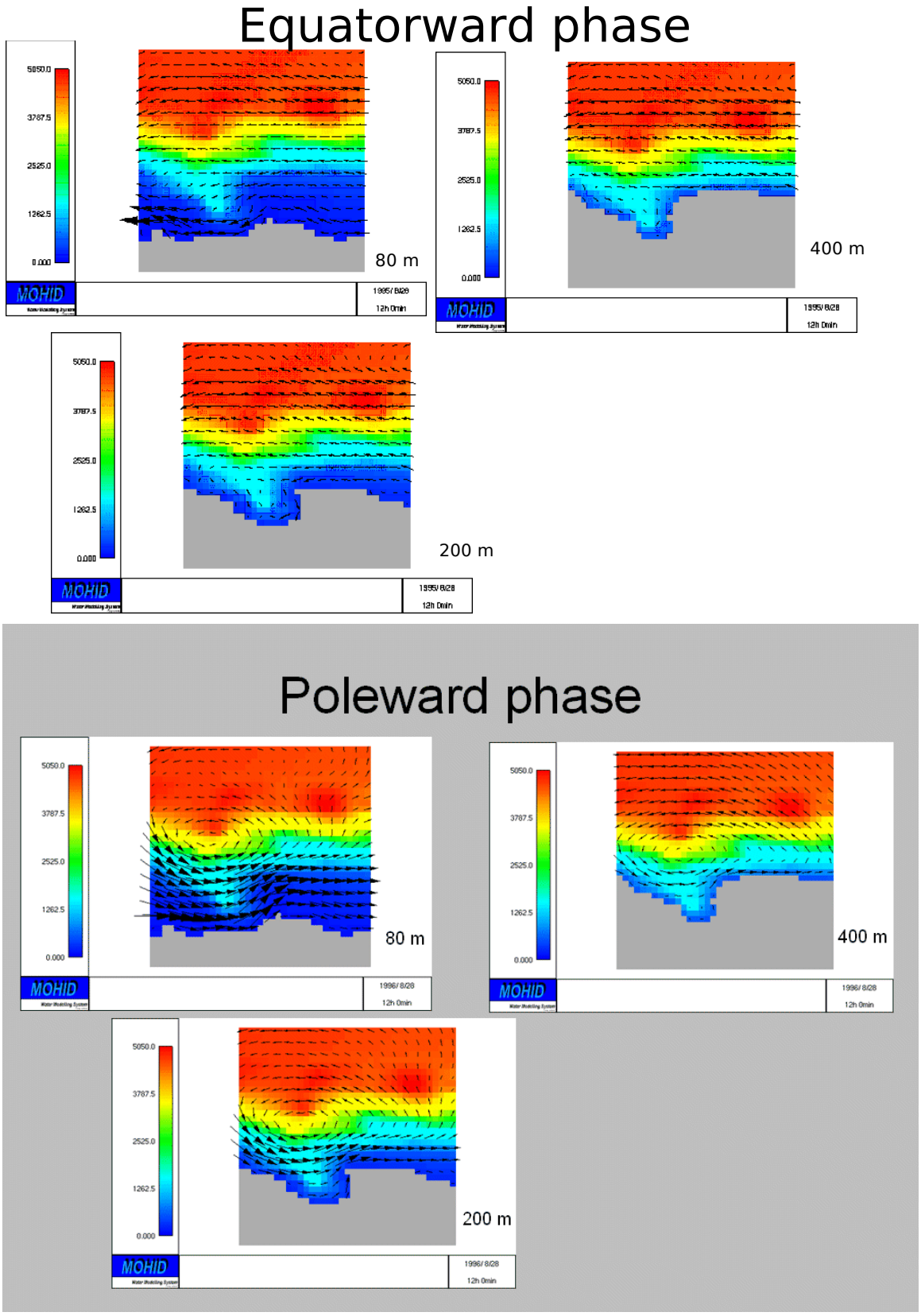

Figure 6: Results of the numerical model for the “equatorward” and “poleward” phases.

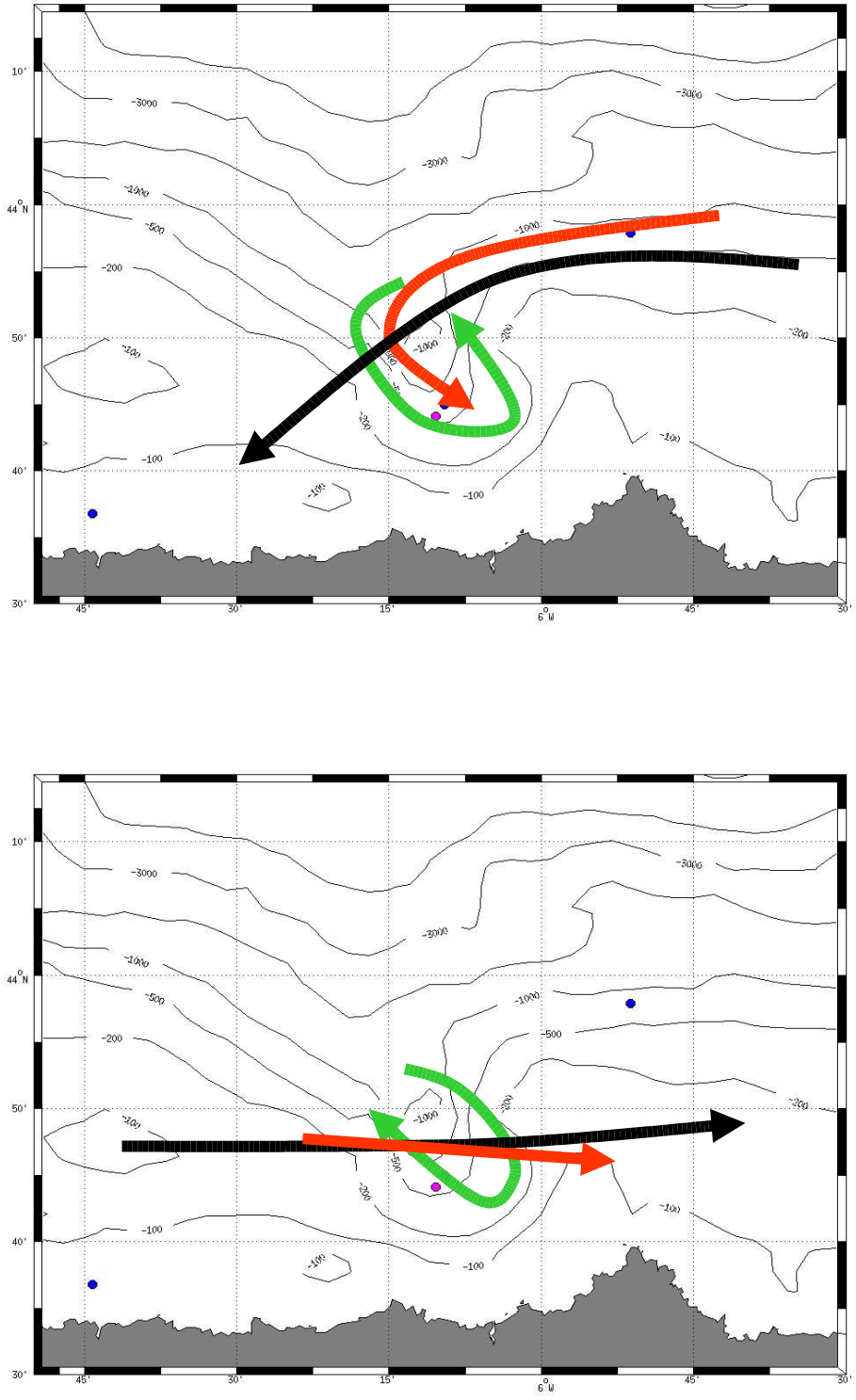

Figure 7: Schema of the obtained mean patterns of circulation for the “equatorward” phase and the “poleward” phase.